#820

Carbon Vol. 19, No. 6, pp. 405–408, 1981
Printed in Great Britain.

0008–6223/81/060405–04$02.00/0
Pergamon Press Ltd.

OXIDATION EFFECTS ON CTE AND THERMAL SHOCK FRACTURE INITIATION IN POLYCRYSTALLINE GRAPHITES

J. ZHAO,† J. L. WOOD,‡ R. C. BRADT and P. L. WALKER, JR.
Department of Materials Science and Engineering, The Pennsylvania State University, University Park, PA 16802, U.S.A.

(*Received* 2 *April* 1981)

Abstract—The coefficient of thermal expansion (CTE) was measured as a function of oxidation for three commercial fine-grained graphites derived from petroleum cokes and coal tar pitches and fabricated by extrusion, unidirectional molding, and isostatic molding. The CTE was observed to vary with the crystallite size and the preferred orientation and to decrease as much as 20% with increasing oxidation. This CTE decrease was attributed to an increase of the accommodation by Mrozowski cracks enlarged by the oxidation process. Effects on thermal shock fracture initiation were examined by estimating changes in the thermal shock resistance parameter, R. It is concluded that in spite of the continuous decrease in CTE, changes in R with oxidation are not continuous for these graphites. The complexity is a consequence of the different extents to which graphite oxidation affects CTE, strength and the Young's elastic modulus.

INTRODUCTION

In many applications, polycrystalline graphites are utilized at elevated temperatures in oxidizing environments. Under these conditions the graphites experience oxidation and at the same time may be subjected to thermal stresses. The effects of oxidation on the mechanical properties pertinent to thermal shock behavior are well known; strength and elastic moduli both decrease with increasing burn-off. Less is known about the effects of oxidation on the coefficient of thermal expansion, CTE, and in particular how the combination of CTE, strength, and elastic modulus changes affect the thermal shock resistance of graphites during oxidation.

It is well established that the resistance to thermal shock fracture initiation is inversely proportional to the CTE[1]. Considerable research has been completed on measuring the CTE of graphites and in theoretically understanding the factors which determine its magnitude[2–10]. It has been demonstrated that a portion of the lattice expansion can be accommodated by the cleavage microcracks (frequently called Mrozowski cracks) formed on cooling from graphitization temperatures. When crystallite alignment is present, the accommodation is more pronounced in the c-direction than in the a-direction. Consequently, the magnitudes of accommodation are related to the amount of preferred orientation, which in turn for filler–binder systems is usually a function of the average crystallite size. Engle[8] has confirmed that the volume CTE decreases monotonically with increasing L_c for bodies fabricated from needle petroleum cokes or gilsonite coke and coal-tar pitch. Wood *et al.*[11] have observed that the Mrozowski microcracks in polycrystalline graphites are often enlarged by oxidation, which may be expected to increase the accommodations of expansion and lower the CTE. It is the purpose of this investigation to determine the magnitude of the CTE changes with oxidation and to examine the resulting effect on the thermal shock fracture initiation resistance.

2. EXPERIMENTAL

2.1 *Preparation of artifacts*

Three commercial graphites§ were examined in this study. Information on the fillers and forming methods are listed in Table 1. Artifacts were produced by mixing a calcined petroleum coke filler with a coal tar pitch, forming, baking, and subsequently graphitizing.

Experimental methods used to characterize these artifacts have been previously reviewed[12]. Important properties are summarized in Table 2. Crystallite alignment (I_T/I_L) was obtained through X-ray diffraction analysis of the intensity ratio of the (002) diffraction peak in the transverse (T) orientation compared to the longitudinal (L) orientation (see Figs. 1 and 2).

Specimens (76 mm × 25 mm × 6 mm) were cut from the artifacts in the longitudinal orientation for the extruded grade and in the transverse and longitudinal orientations for the molded grades (Fig. 1). For the extruded grade, 580, the longitudinal sample has its long dimension parallel to the extrusion direction. In the molded grade, 3499, the transverse sample has its plane of maximum area perpendicular to the molding direction. The longitudinal sample in the molded grade has its plane of intermediate area perpendicular to the molding direction. For the isostatically molded grade, KK-16, "longitudinal" and "transverse" specimens were cut in orientations corresponding to those for grade 3499 as if KK-16 had been unidirectionally molded in a direction perpendicular to the major surface of the artifact. Dashed lines have been added to Fig. 2 to suggest that

†Currently on leave from Peking Materials and Technology Research Institute, Peking, China.

‡Present address: Bendix Corporation, Brake and Strut Division, South Bend, IN 46620, U.S.A.

§Airco Speer Carbon-Graphite, St. Mary's, PA, U.S.A.

Table 1. Fabrication information for the artifacts

Grade	Filler	Maximum Filler Size (μm)	Forming Process	Artifact Dimensions (cm)
580	Petroleum Coke	200	Extrusion	8.9 x 122
3499	Petroleum Coke	75	Molding	30.5 x 30.5 x 6.4
KK-16	Petroleum Coke	20	Isostatic Molding	30.5 x 15.3 x 5.1

Table 2. Selected properties of the graphites

Grade	Apparent Density gm/cc	Porosity (%) Open	Closed	Total	Mean Macropore Size (μm)	Interlayer Spacing d_{002} (nm)	X-Ray Crystallite Alignment (I_T/I_L)	CTEX10^6 $(°K^{-1})$
580	1.70 ± .004	22.8	1.9	24.7	2-5	.3364	1.62	2.87
3499	1.71 ± .003	17.8	6.4	24.2	5	.3368	2.09	3.80 (L) 4.69(T)
KK-16	1.84 ± .002	12.5	5.9	18.4	1.5	.3370	0.89	5.08(L) 5.58(T)

some preferential alignment of basal planes is expected (as a function of forming direction) for samples of 3499 and 580. It should be emphasized that, for the molded materials, "longitudinal" does not refer to a specimen with its long dimension parallel to the molding direction. Rather, "longitudinal" is used to refer to the molded specimen with preferred crystallite alignment similar to that for longitudinal specimens of the extruded grade (Fig. 2).

2.2 *Oxidation of artifacts*

As discussed previously[11], specimens were oxidized in flowing dry air at 773 K to various total weight losses up to about 20%. Burn-off rates for the graphites varied from 0.14%/hr for grade 580 to 0.23%/hr for grade 3499 as seen in Table 3. The percentage weight decrease (ΔW) always exceeded the percentage density decrease ($\Delta\rho$) during the specimen oxidation; that is, oxidation resulted in both a decrease in specimen volume and in the specimen density. From a knowledge of starting and final sample volume and sample weight, burn-offs in the spe-

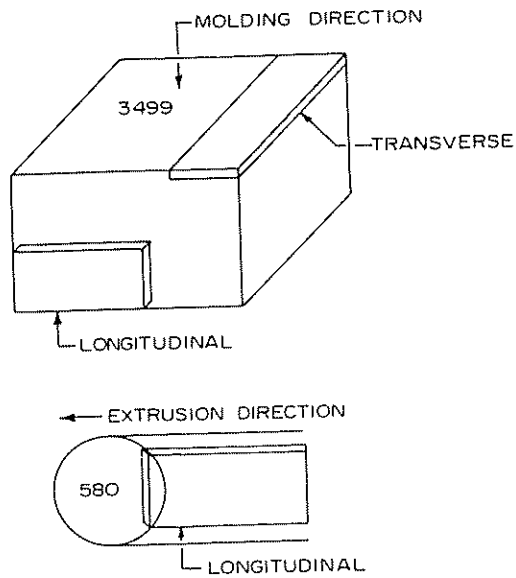

Fig. 1. Artifacts of the graphites with samples cut for subsequent oxidation indicated.

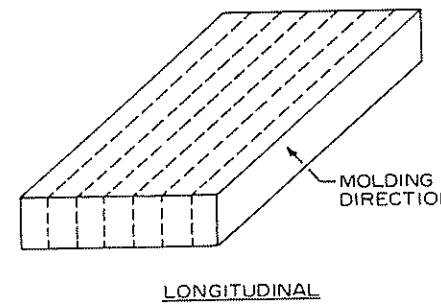

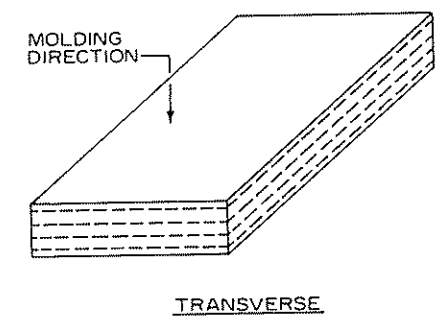

Fig. 2. Longitudinal and transverse specimens showing preferential basal plane alignment (grades 3499 and 580) and molding directions for grade 3499.

Table 3. Information on air oxidation of graphite at 773 K

Grade	Burn-off Rate (%/hr)	-5% Total Burn-Off		-10% Total Burn-Off		-20% Total Burn-Off	
		Δw(%)	Δp(%)	Δw(%)	Δp(%)	Δw(%)	Δp(%)
580	0.14	5.0	0.4	10.3	2.3	19.7	12.4
3499	0.23	6.0	0.6	9.8	4.7	19.8	15.5
KK-16	0.15	4.9	0.7	10.6	6.2	21.3	16.8

cimens remaining could be calculated[11]. These burn-offs were always less than total burn-offs because of decrease in specimen volume.

2.3 *Measurement of CTE*

For CTE measurements, samples 36 mm × 6 mm × 6 mm were cut from the original and oxidized specimens. The long dimension of the samples was parallel to the long dimension of the specimens shown in Fig. 2. CTE was measured for expansion in the long dimension, that is in the direction of preferred crystallite alignment if one exists in the graphite. In a Orton Automatic Recording Dilatometer TXC-6811, the sample was heated at about 200 K/hr between room temperature and 673 K. Insignificant additional sample oxidation occurred at these low temperatures during this time frame. Changes in sample length were transmitted through an alumina pushrod to the plunger of a linear variable differential transformer and then converted to d.c. millivoltage by a transducer exciter–demodulator. The voltage was converted to sample expansion and plotted vs temperature on a recorder. Between room temperature and 673 K, expansion vs temperature was essentially linear. Reproducibility of the CTE measurement was determined on an unoxidized KK-16 specimen. Eleven measurements were made, with the sample removed from the apparatus and replaced after each three measurements. The CTE was $5.58 \pm 0.14 \times 10^{-6}\,K^{-1}$ where the range indicates the 95% confidence limits. For measurements on each oxidized material, at least three separate samples were run. The range of CTE values was in all cases smaller than the size of the data points plotted on the figures.

3. RESULTS AND DISCUSSION

Figure 3 presents results of the CTE as a function of burn-off within the specimen. The CTE is different for each grade. As previously reported by Engle[8], there is no relation between CTE and either the closed or the total porosity for the original samples (Table 2) or for the oxidized samples (Table 4). However, the CTE does decrease as the average interlayer spacing between basal planes within the crystallites of the specimens decreases (Table 2). Since lower interlayer spacing is a result of larger crystallite size[13], CTE decreases as the average crystallite size in the specimen increases, as reported by Engle[8]. For the two graphites where data are available, the CTE at all burn-offs is greater for the transverse specimens than the longitudinal ones. The extent of this difference changes little with burn-off.

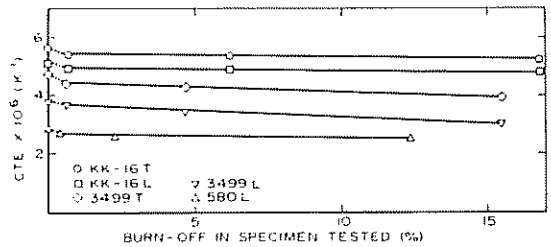

Fig. 3. Change in CTE as a function of burn-off in artifact tested.

Figure 4 presents normalized plots for the decrease in CTE as a function of oxidation. The extent of decrease in CTE with oxidation of the artifact is clearly different for each grade of graphite and even for the longitudinal

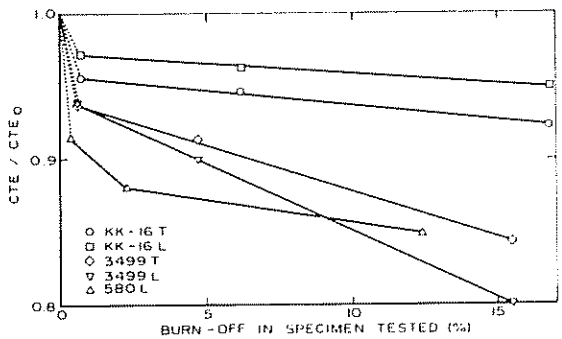

Fig. 4. CTE, normalized to the as-received value, as a function of burn-off in the artifact tested.

Table 4. Change in porosity of the graphites upon oxidation

Grade	Porosity (%)											
	Open				Closed				Total			
	0%	~5%	~10%	~20%	0%	~5%	~10%	~20%	0%	~5%	~10%	~20%
3499	17.8	17.5	22.5	31.5	6.4	6.4	4.8	2.7	24.2	23.9	27.3	34.2
KK-16	12.5	12.5	19.4	30.5	5.9	5.9	4.1	1.8	18.4	18.4	23.5	32.3
580	22.8	22.9	25.3	33.6	1.9	1.8	1.3	0.6	24.7	24.7	26.6	34.2

Table 5. Calculated R values, °K. resistance to thermal shock fracture initiation

	Total Burn-Off (%)			
Grade	0	5	10	20
580	765	559	932	517
3499L	528	449	503	843
3499T	764	640	741	1514
KK16L	1001	803	1014	1101
KK16T	906	709	846	826

specimens as compared to transverse ones of the same grade. As expected, decreases in CTE do not correlate with increases in total pore volume nor with decreases in closed pore volume in the artifacts as a result of oxidation (Table 4). Neither do the fractional decreases in CTE correlate with the magnitude of the CTE in the original artifacts.

Changes in CTE with oxidation are in marked contrast, for the most part, to changes in Young's moduli (E) and shear moduli (G) measured on the same specimens[11]. In contrast to the CTE results, the decrease in moduli with increasing oxidation correlated well with the increase in total porosity for a particular graphite grade. Also the normalized decrease in E and G with carbon burn-off was greater than the decrease in CTE. For example, for the samples with a total burn-off of about 20%, E/E_0 and G/G_0 were about 0.3, compared to values no smaller than 0.8 for CTE/CTE$_0$. There was one similarity between the changes of CTE and E and G with oxidation[11]. That is, for all three properties, significant decrease occurred at low specimen burn-offs. For example, as seen in Fig. 4, CTE/CTE$_0$ decreases most sharply for specimen burn-offs up to about 0.7%.

After Kingery, the thermal shock fracture initiation resistance parameter for materials of comparable thermal properties is R, when:

$$R(^\circ K) = \frac{\sigma_f(1-\nu)}{\alpha E}. \quad (1)$$

The σ_f term represents the strength, α is the CTE, E is Young's elastic modulus, and ν is Poisson's ratio. Using data[11, 12, 14] for these same graphites for σ_f, ν, and E yields the results summarized in Table 5 for changes in R with oxidation. No continuous trend is evident in this summary. However, several consistent changes are evident, namely that on the initial burn-off there is a decrease in the R factor, after which it increases to varying degrees. It is interesting to examine which factors cause these R variations.

The initial decrease in R, an indication of a drop in resistance to thermal shock, is a combination of rapid decreases in σ_f, CTE, and E at the beginning of oxidation. However, the σ_f decrease is the most rapid, causing the early R decrease. Rounthwaite *et al.*[15] have similarly noted for petroleum coke–coal tar pitch graphites that the strength decreases more rapidly than the elastic modulus during burn-off in CO_2. For example, a 20% burn-off reduces $\sigma_f/\sigma_0 \approx 0.17$, but $E/E_0 \approx 0.22$. They also observed a 60% decrease in the electrical conductivity with only a 20% burn-off. Obviously, many physical properties, as well as derived descriptive parameters such as R, exhibit large decreases on initial oxidation of graphite, whether in air or in CO_2.

After the initial burn-off, the R values recover for each of the graphites and in several instances actually exceed their initial values. This is a consequence of the different rates of decrease of σ_f, α and E and their functional relation to R. Whereas all of the properties decrease rapidly on initial burn-off, both σ_f and α appear to decrease less rapidly in the later stages.

Acknowledgements—This study was made possible by a grant from Airco Speer Carbon-Graphite to support the Ph.D. thesis research (for J.L.W.) and by support from the government of China (for J.Z.).

REFERENCES

1. W. D. Kingery, *J. Am. Cer. Soc.* **38**, 3 (1955).
2. D. Ali, E. Fitzer and A. Ragoss, *Proc. 1st Ind. Conf. Carbon and Graphite*, p. 135. Society of Chemical Industry, London (1958).
3. M. Inagaki and T. Noda, *Carbon* **1**, 86 (1963).
4. A. L. Sutton and V. C. Howard, *J. Nucl. Mater.* **7**, 58 (1962).
5. R. J. Price and J. C. Bokros, *J. Appl. Phys.* **36**, 1897 (1965).
6. L. D. Loch and A. E. Austin, *Proc. 1st and 2nd Carbon Conf.*, p. 65. University of Buffalo (1956).
7. J. M. Hutcheon and M. S. T. Price, *Proc. 4th Carbon Conf.*, p. 645. Pergamon Press, Oxford (1960).
8. G. B. Engle, *Carbon* **8**, 485 (1970).
9. G. B. Engle, *Carbon* **12**, 291 (1974).
10. G. W. Hollenberg and R. Ruh, *AIP Conf. Proc.*, No. 17, p. 241 (1973).
11. J. L. Wood, R. C. Bradt and P. L. Walker, Jr., *Carbon* **18**, 179 (1980).
12. J. L. Wood, R. C. Bradt and P. L. Walker, Jr., *Carbon* **18**, 169 (1980).
13. H. Takahashi, H. Kuroda and H. Akamatu, *Carbon* **2**, 432 (1965).
14. J. Zhao, J. L. Wood, R. C. Bradt and P. L. Walker, Jr., *Carbon* **19**, 61 (1981).
15. C. Rounthwaite, G. A. Lyons and R. A. Snowdon, *Proc. 2nd Ind. Conf. Carbon and Graphite*, p. 299. Society of Chemical Industry, London (1966).
16. A. R. Ubbelohde and F. A. Lewis, *Graphite and its Crystal Compounds*. Clarendon Press, Oxford (1960).